Int. J. Electron. Commun. (AEÜ) 175 (2024) 155062

Contents lists available at ScienceDirect

Int. J. Electron. Commun. (AEÜ)

journal homepage: www.elsevier.com/locate/aeue

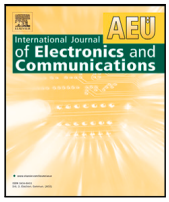

Regular paper

# Ka-band diplexer design based on half-mode groove gap waveguide

Stephan Marini [a,*], Miguel Ferrando Rocher [b], Aitor Morales Hernández [a], Encarnación Gimeno Nieves [a], Alejandro Jorge López [c], Vicente E. Boria [c]

[a] Department of Physics, Systems Engineering and Signal Theory, University of Alicante, 03690 Alicante, Spain
[b] Antennas and Propagation Laboratory (APL), Universitat Politècnica de València, 46022 València, Spain
[c] Microwave Applications Group (GAM-iTEAM), Universitat Politècnica de València, 46022 València, Spain

ARTICLE INFO

*Keywords:*
Gap waveguide technology
Groove gap waveguides
Satellite communications
Waveguide diplexer

ABSTRACT

This paper shows the practical design of a Ka-band tuning-less diplexer in half-mode groove gap waveguide (HM-GGW) technology for multi-beam satellite applications. This new technology can be easily manufactured, since it lets the design of two separate metallic pieces: one for the cover with periodic pins, and another one for the half-groove gap waveguide structure. The proposed diplexer is composed of two bandpass HM-GGW filters, an H-plane T-junction and the corresponding transitions to the input/output WR28 rectangular ports. To illustrate how this technology can be applied, a prototype has been successfully fabricated, showing in-band measured return and insertion losses of 21 dB and 0.87 dB in the lower band, 16 dB and 0.86 dB in the upper band, and a good isolation level (better than 32.5 dB) in the whole operational frequency range.

## 1. Introduction

Microwave diplexer is a device used in high frequency communication systems to combine or separate two frequency bands. The function of this component is to enable the efficient sharing and separation of different frequency bands, optimizing spectrum utilization and minimizing interference between transmitting and receiving channels. A diplexer allows the sharing of a common antenna or transmission line with the receiver of communication systems in satellite payloads and Earth stations [1,2].

A typical approach for designing a diplexer involves the individual design of each channel filter, followed by their combination using a distribution network. This network can take the form of a manifold or a 3-port T-junction with a common port [3–10]. For millimeter-band frequencies some specific considerations, due to the higher operational frequencies involved, are necessary. It is worth noting that the analysis, design and manufacturing of passive hardware can be more challenging due to the smaller dimensions, major effects of manufacturing tolerances, higher losses and increased sensitivity to parasitic effects. In this context, a very good candidate for realization diplexers to operate at these higher frequencies is the gap technology [11]. Gap waveguides (GWs) offer a significant advantage in mitigating the issue of imperfect contact and alignment between various metal layers or metal parts, achieving components with high-quality factor [12]. Groove gap waveguide (GGW) is a particular type of gap technology that has been implemented in the development of power dividers [13], filters [14–17], diplexers [18–20] as well as single and multiband antennas [21–25].

HM-GGW is a new waveguide that was introduced recently in [26]. This innovative waveguide, functioning similarly to a conventional GGW, replaces half of its width with a homogeneous cover of metal pins generating a high impedance surface. In this way, the size and footprint of a HM-GGW component is reduced more than 20% respect to the same GGW one, and still being a gap technology, it does not need a perfect contact between metal pieces that are separated by a fixed small air gap. While, in a conventional waveguide, an identical design featuring an air gap would be unfeasible and would face compatibility issues related to roughness, misalignment, and sealing problems. Furthermore, HM-GGW technology offers a great advantage in terms of manufacturing, since it allows the design of separate parts in a simplified machining process: the cover with metal periodic pins, and, on the other hand, the half-groove waveguide on a metal bottom piece. The absence of cavities, transitions, or bends adjacent to the pins considerably streamlines the manufacturing process. To date, HM-GGW technology has been used in the design of different components such as filters [27], couplers [28], and antennas [29,30].

In this work a Ka-band tuning-less diplexer based on HM-GGW is designed and fabricated. To the authors' knowledge, it is the first time that this technology has been used for implementing this passive

* Corresponding author.
*E-mail addresses:* smarini@ua.es (S. Marini), miguel.ferrando@upv.es (M.F. Rocher), aitor.morales@ua.es (A.M. Hernández), encarna.gimeno@ua.es (E.G. Nieves), ajorlop@iteam.upv.es (A.J. López), vboria@dcom.upv.es (V.E. Boria).

https://doi.org/10.1016/j.aeue.2023.155062
Received 7 November 2023; Accepted 11 December 2023
Available online 19 December 2023

**Table 1**
Desired HM-GGW diplexer specifications.

| Parameter | Value |
|---|---|
| Central frequency | Channel 1: 28 GHz, channel 2: 29.4 GHz |
| Bandwidth | 800 MHz |
| Return losses | >20 dB |
| Insertions losses | <0.9 dB |

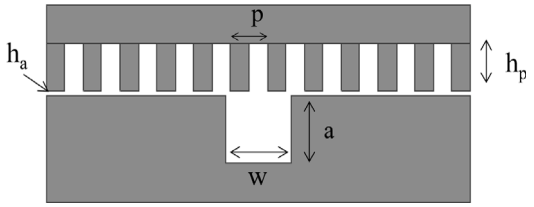


**Fig. 1.** Generic HM-GGW cross-section.

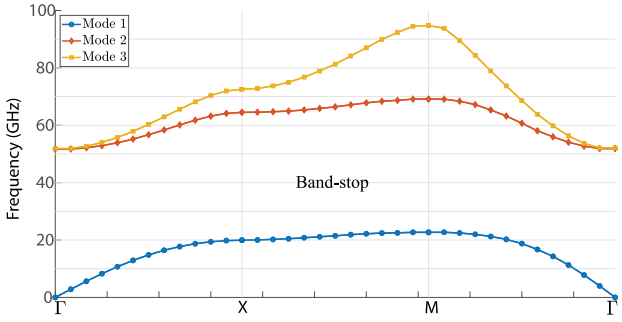


**Fig. 2.** Dispersion diagram of the metallic periodic pins cover. 1 × 1 mm square pins with period of 2 mm are used.

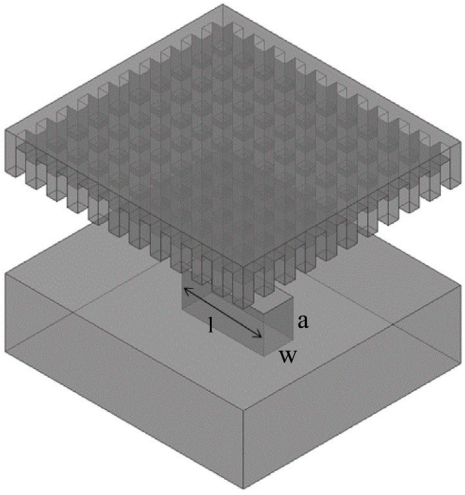


(a)

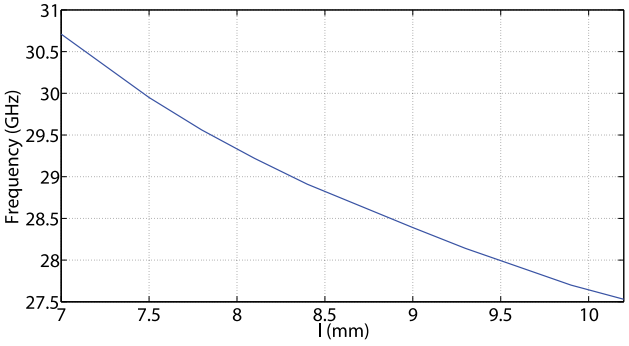


(b)

**Fig. 3.** Half-Mode groove gap waveguide resonator (fixed $a$ = 3.55 mm and $w$ = 2.85 mm). (a) Cavity structure. (b) Resonant frequency versus length of cavity $l$.

component. The diplexer structure is composed by a symmetric T-junction with transitions to WR28 rectangular ports, and two inductive bandpass filters. Table 1 shows the ideal requirements that we have selected as the benchmark for the considered diplexer prototype, which can be summarized as two channel filters of order 4 centered at 28 and 29.4 GHz, respectively, with 800 MHz of bandwidth each one, return losses better than 20 dB and insertion losses below than 0.9 dB. These specifications are generally requirements for multi-beam payloads in space applications [31].

The contents of this work's manuscript are arranged as follows. In Section 2, the structure of the periodic pin cover and HM-GGW cavity are first analyzed. Then the T-junction and the required transitions to WR28 input/outputs ports are designed. Section 3 will be devoted to the analysis of Ka-band HM-GGW bandpass filters wherein inductive irises are employed to control the coupling between cavities. In Section 4, the proposed HM-GGW diplexer is implemented by connecting previously designed bandpass filters to the T-junction under consideration. The results of simulations and measurements are provided. Finally, Section 5 summarizes the main conclusions of this paper.

## 2. Half-mode groove gap resonant cavity and T-junction

Half-mode groove gap waveguide (HM-GGW) is made up of two parallel metallic plates (see Fig. 1). These two parallel metallic plates are separated by a gap $h_a$ lesser than $\lambda/4$, to stop waves from traveling through this air gap. Respect to a classical GGW, the width of the groove $w$ is the same than the classical one, whereas the groove height $a$ is the half one, so a more compact structure is obtained, while half $TE_{10}$-like mode is propagating in the groove.

The metallic pin dimensions and gap size are chosen to achieve a stop-band covering the specified frequency working band. Then, the first step is the implementation of the periodic metal pins cover. A period of $p$ = 2 mm of square pins with a cross section of 1 × 1 mm, pin height of $h_p$ = 2.5 mm (approximately $\lambda_0/4$ at 30 GHz) and air gap of $h_a$ = 0.2 mm, are used to produce the high impedance surface. The dispersion diagram of Fig. 2 shows that these values ensure a high band-stop for Ka-band application. This band-gap extends from 22.7 GHz to roughly 51.7 GHz, the frequency at which higher order modes start to propagate.

Fig. 3a shows the half-mode groove gap rectangular cavity structure, which will be used as resonator in the filter and diplexer designs of Section 3 and Section 4. The width and height of the HM-GGW cavity are fixed to $w$ = 2.85 mm and $a$ = 3.55 mm, respectively, and the pins cover previously designed is used. The resonant frequency of the dominant cavity mode in function of cavity length $l$ is computed using the eigenmode analysis of Ansys high frequency structure simulator (HFSS)[1] and it is shown in Fig. 3b.

Finally, the proposed configuration of a symmetrical T-junction is represented in Fig. 4. The input common port and the two channels output ports are WR28 rectangular apertures located in the bottom piece of the structure, and all of them are interconnected with the same transition to the groove waveguide. This transition is simple and it is composed by a rectangular iris terminated in the groove with

[1] HFSS, Copyright 2021 ANSYS, Inc. All rights reserved. [Online]. Available: https://www.ansys.com/products/electronics/ansys-hfss.

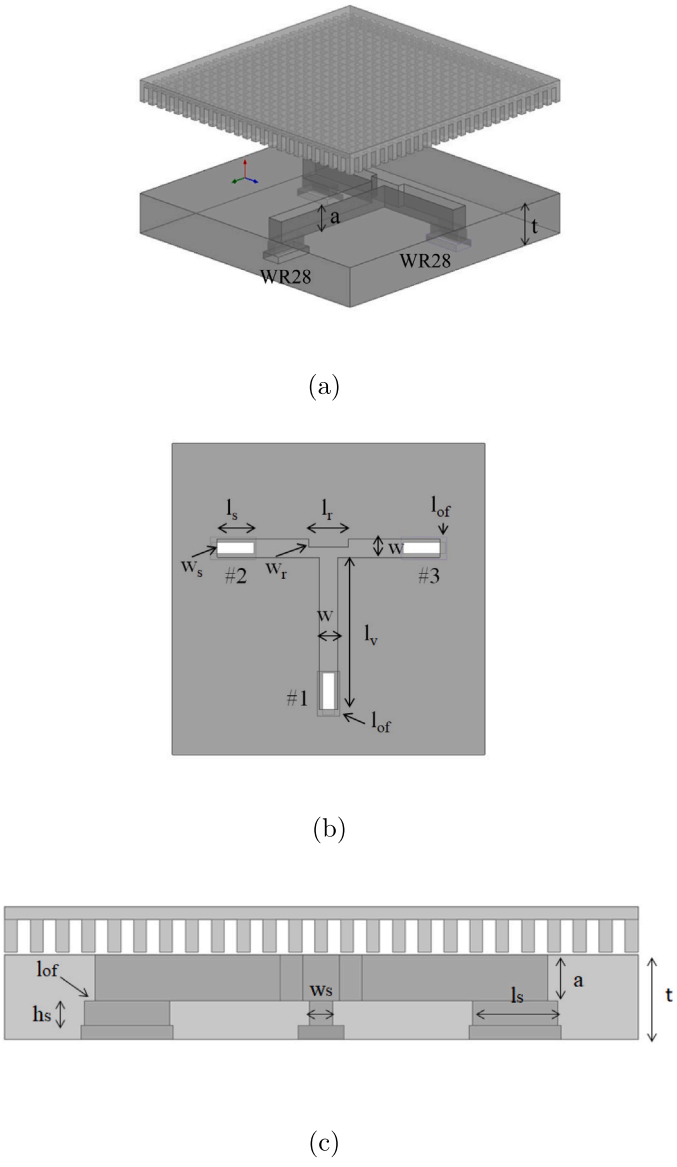


**Fig. 4.** T-junction structure with transition to WR28 input and output ports. (a) Three-dimensional view. (b) top view. (c) lateral view.

**Table 2**
Dimensions of transition parameters (in mm).

| $w_s$ | $l_s$ | $h_s$ | $l_{of}$ | $t$ |
|---|---|---|---|---|
| 1.94 | 6.6 | 2.2 | 1.056 | 6.55 |

a slot width of $w_s = 1.94$ mm, a slot length of $l_s = 6.6$ mm, and thickness of $h_s = 2.2$ mm (the total thickness $t$ is 6.55 mm). It is important to highlight that input and output WR28 ports are offset of $l_{of} = 1.056$ mm from the end of the groove waveguide (see Fig. 4). All transition parameters are summarized in Table 2.

Fig. 5 exhibits the frequency response of the optimized T-junction transition with vertical arm of length $l_v = 24$ mm and horizontal arm of total length equal to 35 mm, where a centered slit of width $w_r = 1.25$ mm and length $l_r = 6.3$ mm is also added to improve the response. As can be seen, this simple transition guarantees good matching in the desired bandwidth ($|S_{11}|$ better than 19 dB), and allows to equally distribute the input power into the two T-junction branches.

## 3. Half-mode groove gap bandpass filter

After completing the initial design of the T-junction, two fourth-order HM-GGW inductive bandpass filters with Chebyshev response have been synthesized, using the classical theory based on coupled resonators [1]. The filters are working at a central frequency of 28 and 29.4 GHz, with 20 dB return losses in a bandwidth of 800 MHz, meeting the desired specifications of Table 1. From the Chebyshev lowpass prototype parameters ($g_0 = 1$, $g_1 = 0.9314$, $g_2 = 1.292$, $g_3 = 1.5775$, $g_4 = 0.7628$, and $g_5 = 1.221$), the following external quality factor and coupling coefficients can be obtained [32]:

$$Q_{ext} = \frac{g_0 g_1}{FBW} = \frac{g_4 g_5}{FBW} = 34.24 \tag{1}$$

$$M_{1,2} = M_{3,4} = \frac{FBW}{\sqrt{g_1 g_2}} = \frac{FBW}{\sqrt{g_3 g_4}} = 0.025 \tag{2}$$

$$M_{2,3} = \frac{FBW}{\sqrt{g_2 g_3}} = 0.019 \tag{3}$$

where $FBW$ is the fractional bandwidth of the filter, and the values are computed for the filter centered at 29.4 GHz (upper band channel). Then, full-wave electromagnetic simulations have been employed to extract $M_{i,i+1}$ and $Q_{ext}$ as

$$M_{i,i+1} = \frac{f_2^2 - f_1^2}{f_2^2 + f_1^2} \tag{4}$$

$$Q_{ext} = \frac{f_0}{\Delta f_{\mp 90}} \tag{5}$$

where coupling coefficient between consecutive resonators (see the inset of Fig. 6a) is computed from the resonant frequencies $f_1$ and $f_2$, by varying the height $h$ of the central coupling iris and fixing the other ones to 3.3 mm. Similarly, external coupling is computed from the singly loaded resonator of Fig. 6b, where $\Delta f_{\mp 90}$ is determined by the frequencies at which the phase shifts of $S_{11}$ parameter is $\pm 90°$ with respect to the absolute value of phase at $f_0$.

A 3D view of a fourth-order HM-GGW bandpass filter is represented in Fig. 7. The half-mode groove gap waveguide's width and height are fixed at $w = 2.85$ mm and $a = 3.55$ mm, respectively. Table 3 summarizes the final iris heights and cavity lengths, whereas all irises have a fixed thickness of 1 mm. Fig. 8 shows the simulated frequency response for both filters with WR28 input/output access ports. In the desired bandwidth of 800 MHz, the return losses are better than 21 dB, and the insertion losses (filters simulated as aluminum as material) are about 0.5 dB at the central frequency, for both filters.

## 4. Half-mode groove gap diplexer

Once the two bandpass filters, the T-junction and the corresponding transitions to the input and output ports have been designed, the HM-GGW tuning-less diplexer can be assembled by joining all these parts (see Fig. 9). The diplexer must now be tuned because of the loading effect that occurs when filters are connected to a T-junction. In this process, we have employed the approach used in [33] for the design of manifold-coupled multiplexers without the aid of any stubs. First of all, in order to reduce the filter interaction, the optimal values of $l_0$, the length distance from the centered slit to the first coupling iris for both arms, is found. This optimal length is selected to minimize the return loss of common port at 28 GHz, when it is analyzed the channel filter centered at 29.4 GHz, and the other way around. Then, the first coupling iris ($h_1$) and the first resonator length ($l_1$) of upper band filter are adjusted in order to recover the electrical response of the standalone filter at its central frequency (29.4 GHz). Once these two dimensions are tuned, the diplexer response in this channel is very similar to the desired one. Next step is to readjust dimensions of the lower band filter, without changing any parameters of the previously tuned ones. As this channel filter has the worst loading effect, the first two coupling

**Table 3**
Dimensions of each filter channel (in mm).

| $f_0$ (GHz) | $l_0$ | $h_1$ | $l_1$ | $h_2$ | $l_2$ | $h_3$ | $l_3$ | $h_4$ | $l_4$ | $h_5$ |
|---|---|---|---|---|---|---|---|---|---|---|
| 28.0 | 6 | 1.598 | 7.287 | 2.313 | 8.336 | 2.457 | 8.336 | 2.313 | 7.287 | 1.598 |
| 29.4 | 6.2 | 1.774 | 6.195 | 2.579 | 7.161 | 2.755 | 7.161 | 2.579 | 6.195 | 1.774 |

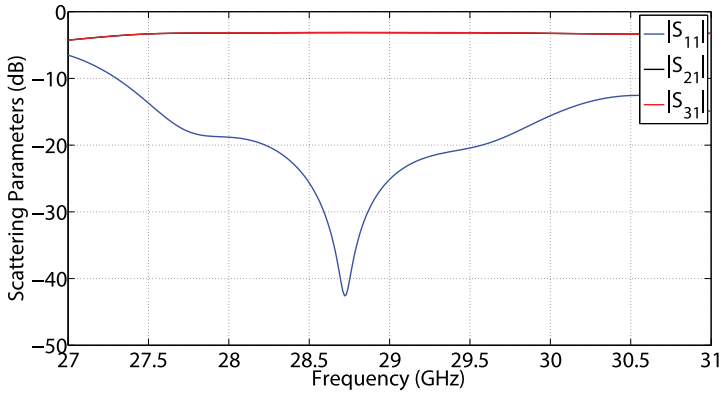


**Fig. 5.** Frequency response of the T-junction.

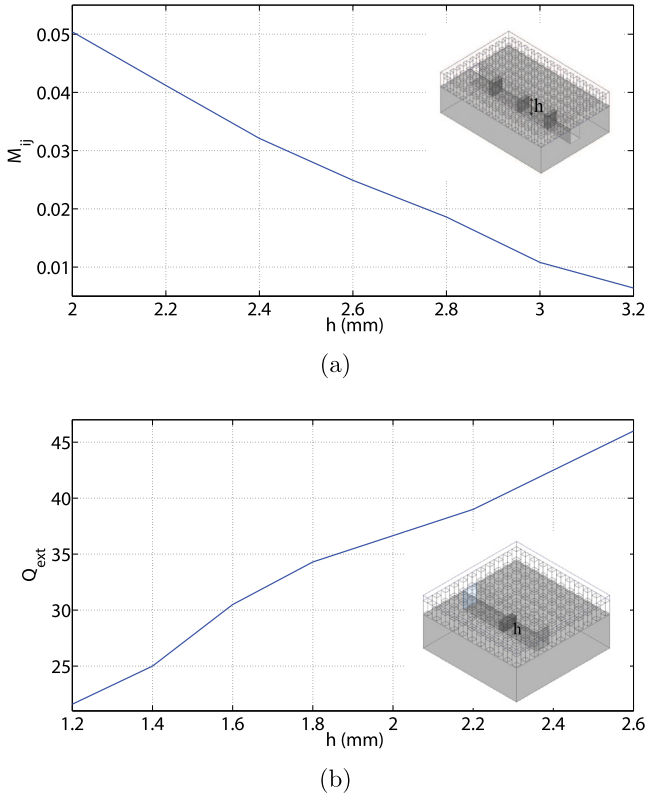


**Fig. 6.** Realization of coupling in HM-GGW filter for the filter centered at 29.4 GHz. (a) Inter cavity coupling coefficient versus iris height $h$. (b) External coupling coefficient versus first/last iris height $h$.

irises and two resonator lengths are now sequentially re-adjusted to recover the response in its channel. Finally, a last fine optimization with adjustment of first coupling and first resonator of both filters, now

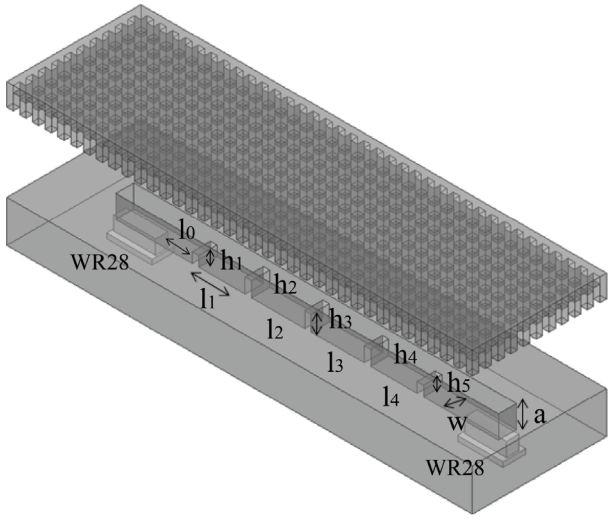


**Fig. 7.** Structure of the fourth-order HM-GGW bandpass filter with the vertical transition to WR28.

in the entire bandwidth of the diplexer, is performed. As a result, this designed diplexer has an overall compact size of 140 × 53 × 15.8 mm$^3$ or 9.5 $\lambda_g$ × 3.6 $\lambda_g$ × 1.08 $\lambda_g$, while all optimized dimensions (see Fig. 10) are summarized in Table 4 . In comparison with the rectangular waveguide diplexer proposed in [10], designed at around 20 GHz, with this technology it is possible to reduce the entire volume of this component by 45%.

The device's frequency response, which satisfies the desired criteria specified in Table 1, is displayed in Fig. 11. Simulated $|S_{11}|$ is better than 22.5 dB, and a minimum insertion loss of 0.55 dB and 0.57 dB at center of each channel is obtained assuming the entire structure is made of aluminum. For experimental verification, an aluminum prototype of the diplexer has been manufactured utilizing a computer numerical control (CNC) Datron M25 milling machine. Fig. 11 compares measured

**Table 4**
Diplexer dimensions in mm ($l_0$ is the length distance from the centered slit to the first coupling iris).

| $f_0$ (GHz) | $l_0$ | $h_1$ | $l_1$ | $h_2$ | $l_2$ | $h_3$ | $l_3$ | $h_4$ | $l_4$ | $h_5$ | $l_5$ |
|---|---|---|---|---|---|---|---|---|---|---|---|
| 28 | 4.6 | 1.201 | 6.77 | 2.349 | 8.398 | 2.457 | 8.336 | 2.313 | 7.287 | 1.598 | 6 |
| 29.4 | 6.4 | 1.841 | 5.978 | 2.579 | 7.161 | 2.755 | 7.161 | 2.579 | 6.195 | 1.774 | 6.2 |

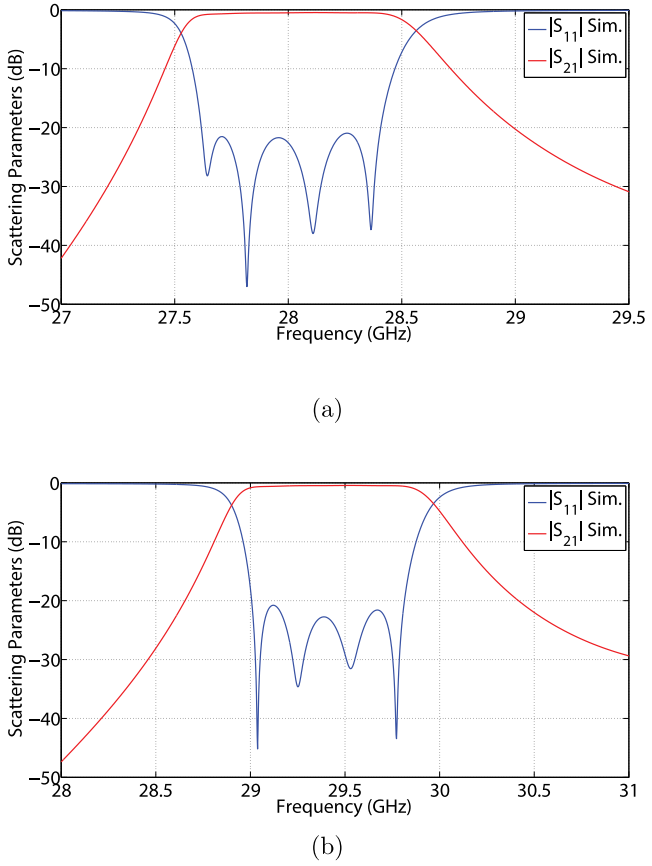


**Fig. 8.** Simulated HM-GGW bandpass filter frequency responses. (a) Filter centered at 28 GHz. (b) Filter centered at 29.4 GHz.

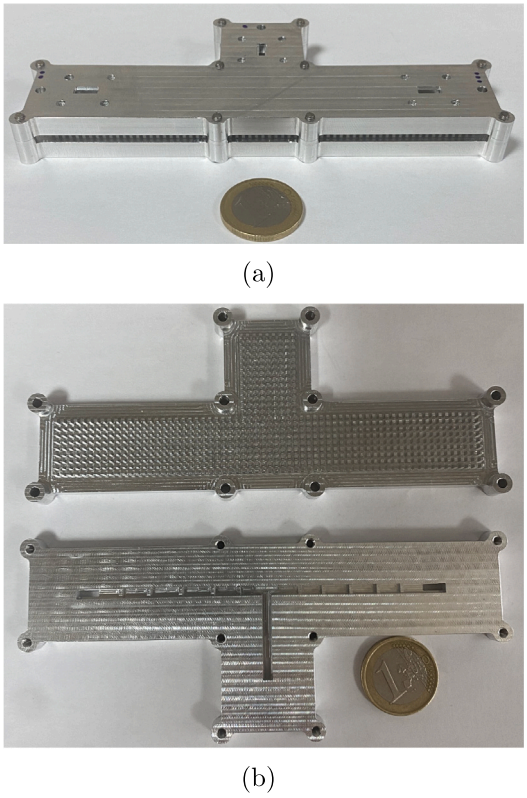


**Fig. 9.** View of the designed (and manufactured) HM-GGW diplexer. (a) 3D bottom view with WR28 rectangular input/output ports. (b) Internal top view of the cover with metal periodic pins and the HM-GGW piece.

and simulated results with an high agreement. As it can be seen, there is a shift of 100 MHz in the center frequency of the measured channel responses, as well as higher insertion losses (0.87 and 0.86 dB, respectively). Moreover, measured return losses are better than 21 dB in the lower channel and better than 16 dB in the upper channel. All these issues are directly attributed to a small inaccuracy of the employed in-house manufacturing process (manufacturing tolerances of 50 microns). The simulated E-field distribution within the HM-GGW diplexer, at center frequencies of the lower- and upper-band filter channels are illustrated in Fig. 12. It can be clearly observed the filtering of the two diplexer bands.

Fig. 13 represents the isolation level between diplexer output ports, where it is shown that measured $|S_{32}|$ is better than 32.5 dB in the in-band response. This value meets the requirements for two contiguous diplexer channels. Respect to the group delay, this is almost flat in the bandwidth of both channels (see Fig. 14). Note also the presence of the same shift of 100 MHz between measurements and simulations of the group delay, due to the fabrication tolerances mentioned above.

Finally, Table 5 provided a comparison between the designed component and reported prototypes at K- and Ka-band given in the literature. Diplexers based on rectangular waveguide, GGW and also SIW technology are considered. The proposed tuning-less device performs comparably or even better with respect to return losses and insertion losses (at $f_0$), meanwhile the isolation between ports can be improved using higher-order HM-GGW filters. All these characteristics make this diplexer based on HM-GGW a technology well-suited for mm-wave band satellite applications.

## 5. Conclusion

In this paper, a Ka-band tuning-less half-mode groove gap diplexer has been successfully designed. Its configuration consists in two HM-GGW bandpass filters directly connected by an H-plane T-junction. Transitions of the HM-GGW to WR28 input and outputs ports are also included in the bottom piece of the proposed solution. The performance of this device has been well verified with the commercial software Ansys HFSS, and by measurements of a prototype manufactured with a computer numerical control (CNC) machine. The overall agreement between measurements and simulation is high. This good electrical behavior demonstrates that HM-GGW is an attractive technology for the design of high frequency components, thus helping to reduce its original size and footprint. Furthermore, because cavities, discontinuities and/or transitions are not positioned next to the pins, HM-GGW offers a significant advantage in terms of manufacturing over classical gap waveguide technology.

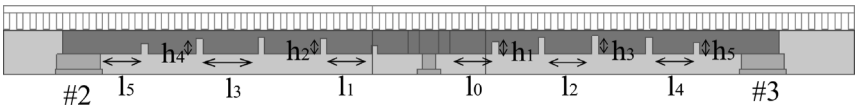


**Fig. 10.** Lateral view of HM-GGW diplexer with parameters defined in Table 4.

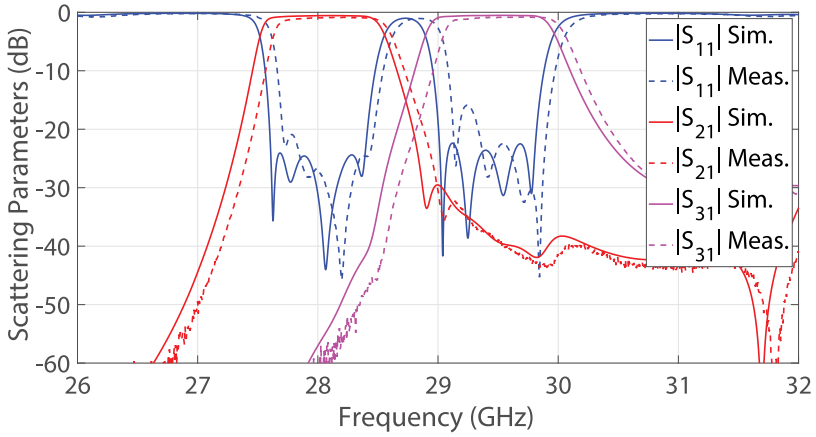


**Fig. 11.** Simulated and measured HM-GGM diplexer frequency responses.

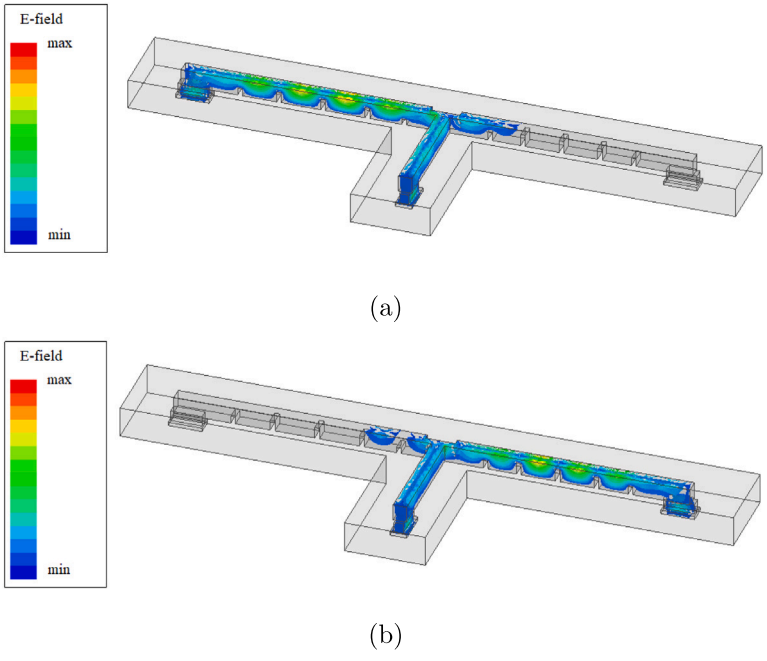


**Fig. 12.** Simulated E-field distributions within the HM-GGW diplexer. (a) 28 GHz. (b) 29.4 GHz.

**Table 5**
Comparison of performances of manufactured and referenced diplexers at K- and Ka-band.

| Ref. | Tech. | Order | FBW | $f_{c1}/f_{c2}$ (GHz) | Insertion loss (dB) | Return loss (dB) | Isolation (dB) |
|---|---|---|---|---|---|---|---|
| [4] | RW | 6/6 | 1.2%/1.15% | 37.8/39.1 | 0.92 | >19/>20 | >32.5 |
| [5] | RW | 6/6 | 0.9%/0.87% | 38.775/39.475 | 2.0 | >15/>15 | >50 |
| [10] | RW | 4/4 | 1.2%/1.2% | 19.82/20.082 | 0.39/0.37 | >20/>20 | >20 |
| [19] | GGW | 4/4 | 3.5%/2.9% | 14/15.5 | 0.8/0.8 | >20/>20 | >35 |
| [20] | GGW | 7/7 | 2.3%/2.2% | 28.21/29.21 | 0.9/0.9 | >13/>13 | >45 |
| [34] | SIW | 5/5 | 2%/1.9% | 20/21 | 2.75/3.05 | >14.65/>13 | >37 |
| This work | HM-GGW | 4/4 | 2.86%/2.72% | 28.0/29.4 | 0.87/0.86 | >21/>16 | >32.5 |

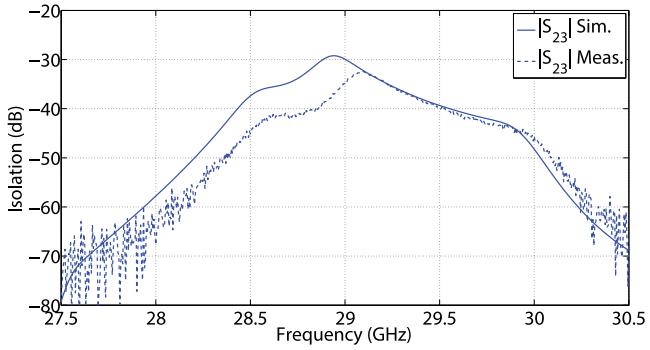


**Fig. 13.** Isolation (module of $S_{23}$ parameter) between diplexer ports.

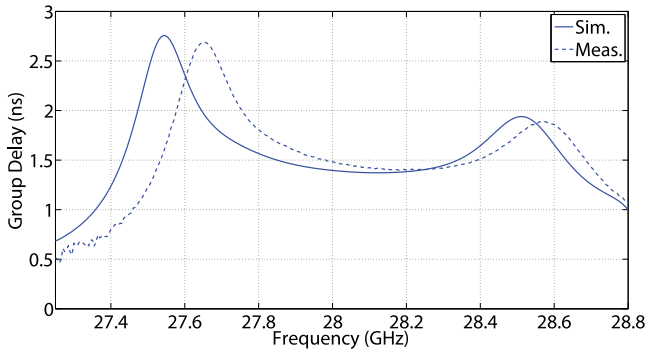


(a)

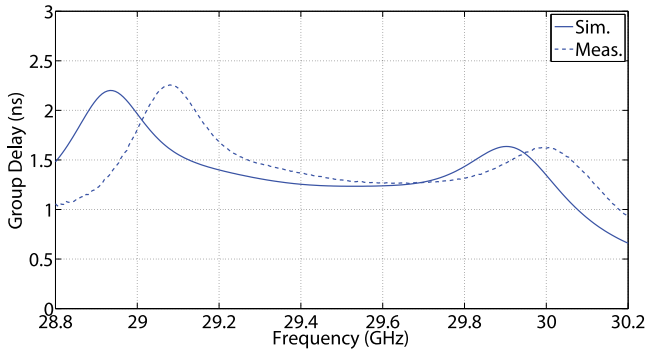


(b)

**Fig. 14.** Group delay. (a) Lower diplexer channel. (b) Upper diplexer channel.

## CRediT authorship contribution statement

**Stephan Marini:** Investigation, Supervision, Writing – original draft, Writing – review & editing. **Miguel Ferrando Rocher:** Supervision, Validation. **Aitor Morales Hernández:** Investigation. **Encarnación Gimeno Nieves:** Investigation. **Alejandro Jorge López:** Investigation, Validation. **Vicente E. Boria:** Supervision.

## Declaration of competing interest

The authors declare that they have no known competing financial interests or personal relationships that could have appeared to influence the work reported in this paper.

## Data availability

No data was used for the research described in the article.

## Acknowledgments

The authors would like to thank Dr. P. Soto Pacheco, Technical University of Valencia, for the fruitful discussions on strategy design of the diplexer, and the Antennas and Propagation Lab (APL – iTEAM UPV) for the fabrication of such device prototype. This work was supported by MCIN/AEI/10.13039/501100011033 and by "ERDF A way of making Europe", through the Sub-Projects C43 and C41 of the Coordinated Projects PID2022-136590OB, and by the University of Alicante, Spain under the project GRE20-06A.

## References

[1] Cameron RJ, Kudsia CM, Mansour RR. Microwave filters for communication systems: Fundamentals, design, and applications. John Wiley & Sons; 2018.
[2] Uher J, Bornemann J, Rosenberg U. Waveguide components for antenna feed systems: Theory and CAD. Artech House; 1993.
[3] Morini A, Rozzi T. Analysis of compact E-plane diplexers in rectangular waveguide. IEEE Trans Microw Theory Tech 1995;43(8):1834–9.
[4] Rong Y, Yao H-W, Zaki KA, Dolan TG. Millimeter-wave Ka-band H-plane diplexers and multiplexers. IEEE Trans Microw Theory Tech 1999;47(12):2325–30.
[5] Shen T, Zaki KA, Dolan TG. Rectangular waveguide diplexers with a circular waveguide common port. IEEE Trans Microw Theory Tech 2003;51(2):578–82.
[6] Ofli E, Vahldieck R, Amari S. Novel E-plane filters and diplexers with elliptic response for millimeter-wave applications. IEEE Trans Microw Theory Tech 2005;53(3):843–51.
[7] San Blas AA, Boria VE, Gimeno B, Cogollos S. Design of compensated multiport waveguide junctions considering mechanization effects. AEU-Int J Electron Commun 2015;69(1):328–31.
[8] Teberio F, Arregui I, Soto P, Laso MA, Boria VE, Guglielmi M. High-performance compact diplexers for Ku/K-band satellite applications. IEEE Trans Microw Theory Tech 2017;65(10):3866–76.
[9] Melgarejo JC, Ossorio J, Cogollos S, Guglielmi M, San-Blas ÁA, Valencia-Sullca JF, et al. A new family of reconfigurable waveguide filters and diplexers for high-power applications. IEEE Access 2023;11:25102–19.
[10] Ossorio J, Melgarejo JC, Cogollos S, Boria VE, Guglielmi M. Waveguide quadruplet diplexer for multi-beam satellite applications. IEEE Access 2020;8:110–6.
[11] Kildal P-S, Alfonso E, Valero-Nogueira A, Rajo-Iglesias E. Local metamaterial-based waveguides in gaps between parallel metal plates. IEEE Antennas Wirel Propag Lett 2008;8:84–7.
[12] Rajo-Iglesias E, Ferrando-Rocher M, Zaman AU. Gap waveguide technology for millimeter-wave antenna systems. IEEE Commun Mag 2018;56(7):14–20.
[13] Alfonso E, Baquero M, Valero-Nogueira A, Herranz J, Kildal P-S. Power divider in ridge gap waveguide technology. In: Proceedings of the fourth European conference on antennas and propagation (EuCAP). IEEE; 2010, p. 1–4.
[14] Baquero-Escudero M, Valero-Nogueira A, Ferrando-Rocher M, Bernardo-Clemente B, Boria-Esbert VE. Compact combline filter embedded in a bed of nails. IEEE Trans Microw Theory Tech 2019;67(4):1461–71.
[15] Wu L, Wu Y, Cheng X, Huang R, Wang W. Design of dual-mode dual-band filter based on multilayer groove gap waveguide. AEU-Int J Electron Commun 2024;173:154975.

[16] Máximo-Gutiérrez C, Hinojosa J, Alvarez-Melcon A. Design of evanescent mode band-pass filters based on groove gap waveguide technology. AEU-Int J Electron Commun 2023;164:154628.
[17] Morales-Hernández A, Sánchez-Soriano MÁ, Ferrando-Rocher M, Marini S, Boria VE. In-depth study of the corona discharge breakdown thresholds in groove gap waveguides and enhancement strategies for inductive bandpass filters. IEEE Access 2022;10:129149–62.
[18] Rezaee M, Zaman AU. Realisation of carved and iris groove gap waveguide filter and E-plane diplexer for V-band radio link application. IET Microw Antennas Propag 2017;11(15):2109–15.
[19] Zarifi D, Shater A, Ashrafian A, Nasri M. Design of ku-band diplexer based on groove gap waveguide technology. Int J RF Microw Comput Aided Eng 2018;28(9):e21487.
[20] Vosoogh A, Sorkherizi MS, Zaman AU, Yang J, Kishk AA. An integrated ka-band diplexer-antenna array module based on gap waveguide technology with simple mechanical assembly and no electrical contact requirements. IEEE Trans Microw Theory Tech 2017;66(2):962–72.
[21] Vazquez-Sogorb C, Ferrando-Rocher M, Marini S, Herranz-Herruzo JI. A gap waveguide-based 2 × 2 circularly-polarized monopulse antenna array. In: 2022 16th European conference on antennas and propagation (EuCAP). IEEE; 2022, p. 1–3.
[22] Haghparast AH, Rezaei P. High performance H-plane horn antenna using groove gap waveguide technology. AEU-Int J Electron Commun 2023;163:154620.
[23] Wang J, Wu Y, Wang W, Ma L. Wideband mm-wave high-gain multibeam antenna array fed by 4 × 4 groove gap waveguide butler matrix with modified crossover. AEU-Int J Electron Commun 2022;154:154287.
[24] Chashmi MJ, Rezaei P, Haghparast AH, Zarifi D. Dual circular polarization 2 × 2 slot array antenna based on printed ridge gap waveguide technology in Ka band. AEU-Int J Electron Commun 2022;157:154433.
[25] Ferrando-Rocher M, Herranz-Herruzo JI, Valero-Nogueira A, Bernardo-Clemente B. Full-metal K-Ka dual-band shared-aperture array antenna fed by combined ridge-groove gap waveguide. IEEE Antennas Wirel Propag Lett 2019;18(7):1463–7.
[26] Ferrando-Rocher M, Herranz-Herruzo JI, Valero-Nogueira A, Baquero-Escudero M. Half-mode waveguide based on gap waveguide technology for rapid prototyping. IEEE Microw Wirel Compon Lett 2022;32(2):117–20.
[27] Marini S, Vázquez-Sogorb C, Ferrando-Rocher M, Morales-Hernández A. Inductive bandpass filters based on half-mode groove gap waveguide. In: 2022 Asia-Pacific microwave conference (APMC). IEEE; 2022, p. 761–3.
[28] Ferrando-Rocher M, Herranz-Herruzo JI, Pérez-Guimerá A, Valero-Nogueira A. Quadrature hybrid coupler implemented in half-mode groove gap waveguide. In: 2023 17th European conference on antennas and propagation (EuCAP). IEEE; 2023, p. 1–3.
[29] Ferrando-Rocher M, Herranz-Herruzo JI, Valero-Nogueira A, Baquero-Escudero M. A half-mode groove gap waveguide for single-layer antennas in the millimeter-wave band. IEEE Antennas Wirel Propag Lett 2022;21(12):2402–6.
[30] Ferrando-Rocher M, Herranz-Herruzo JI, Valero-Nogueira A, Marini S. 1× 4 antenna array corporately fed by a novel half-mode groove gap waveguide network. In: 2022 3rd URSI Atlantic and Asia pacific radio science meeting (AT-AP-RASC). IEEE; 2022, p. 1–3.
[31] Fenech H, Amos S, Tomatis A, Soumpholphakdy V. High throughput satellite systems: An analytical approach. IEEE Trans Aerosp Electron Syst 2015;51(1):192–202.
[32] Hong J-SG, Lancaster MJ. Microstrip filters for RF/Microwave applications. John Wiley & Sons; 2004.
[33] Carceller C, Soto P, Boria V, Guglielmi M, Gil J. Design of compact wideband manifold-coupled multiplexers. IEEE Trans Microw Theory Tech 2015;63(10):3398–407.
[34] Kordiboroujeni Z, Bornemann J. K-band backward diplexer in substrate integrated waveguide technology. Electron Lett 2015;51(18):1428–9.